Biochemistry

Article

Cite This: Biochemistry 2019, 58, 3634−3645

pubs.acs.org/biochemistry

Unveiling the Biochemistry of the Epigenetic Regulator SMYD3

Edoardo Fabini,[†,∥,▽] Vladimir O. Talibov,[‡,▽] Filip Mihalic,[‡] Marina Naldi,[†,§] Manuela Bartolini,[†] Carlo Bertucci,[†] Alberto Del Rio,[∥,⊥] and U. Helena Danielson*[,‡,#]

[†]Department of Pharmacy and Biotechnology, Alma Mater Studiorum University of Bologna, Bologna, Italy

[‡]Department of Chemistry − BMC, Uppsala University, Uppsala, Sweden

[§]Center for Applied Biomedical Research (C.R.B.A.), S. Orsola-Malpighi Hospital, Bologna, Italy

[∥]Institute of Organic Synthesis and Photoreactivity (ISOF), National Research Council (CNR), Bologna, Italy

[⊥]Innovamol Consulting Srl, Modena, Italy

[#]Science for Life Laboratory, Uppsala University, Uppsala, Sweden

Supporting Information

ABSTRACT: SET and MYND domain-containing protein 3 (SMYD3) is a lysine methyltransferase that plays a central role in a variety of cancer diseases, exerting its pro-oncogenic activity by methylation of key proteins, of both nuclear and cytoplasmic nature. However, the role of SMYD3 in the initiation and progression of cancer is not yet fully understood and further biochemical characterization is required to support the discovery of therapeutics targeting this enzyme. We have therefore developed robust protocols for production, handling, and crystallization of SMYD3 and biophysical and biochemical assays for clarification of SMYD3 biochemistry and identification of useful lead compounds. Specifically, a time-resolved biosensor assay was developed for kinetic characterization of SMYD3 interactions. Functional differences in SMYD3 interactions with its natural small molecule ligands SAM and SAH were revealed, with SAM forming a very stable complex. A variety of peptides mimicking putative substrates of SMYD3 were explored in order to expose structural features important for recognition. The interaction between SMYD3 and some peptides was influenced by SAM. A nonradioactive SMYD3 activity assay using liquid chromatography-mass spectrometry (LC-MS) analysis explored substrate features of importance also for methylation. Methylation was notable only toward MAP kinase kinase kinase 2 (MAP3K2_K^{260})-mimicking peptides, although binary and tertiary complexes were detected also with other peptides. The analysis supported a random bi−bi mechanistic model for SMYD3 methyltransferase catalysis. Our work unveiled complexities in SMYD3 biochemistry and resulted in procedures suitable for further studies and identification of novel starting points for design of effective and specific leads for this potential oncology target.

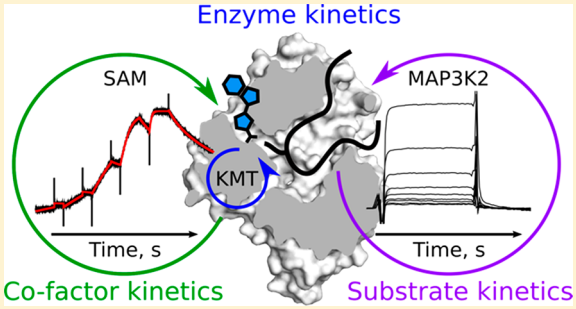

To date, cancer is one of the leading causes of death worldwide and a central topic in pharmaceutical research.[1,2] The intricate pathophysiology of the disease and the complexity of the molecular mechanisms underlying various types of cancer represent a unique challenge for healthcare specialists who strive to establish target-based therapeutic approaches.[2] Among the many mechanisms contributing to cancer onset and progression, epigenome regulation has an important role.[3,4] It involves the dynamics and inheritable post-translational modifications of DNA and nucleosomal proteins. These modifications modulate the chromatin state, eventually leading to its remodeling and the subsequent enhancement or suppression of the activity of the transcription machineries in key promoter regions. Developmental trajectories and phenotypic expression in eukaryotic cells are regulated by this finely tuned machinery that, if impaired, may lead to pathological states including malignancies, metabolic diseases, and neurological disorders.[4,5] Epigenetic enzymes, i.e., the enzymes involved in the epigenetic regulation, work as pairs of writers and erasers to guarantee the spatial-temporal control of gene expression.[6] They are classified according to the targeted amino acid residue and the reaction they catalyze: lysine methyltransferases/demethylases (KMTs/KDTs), arginine methyltransferases/demethylases (RTMs/RDMs), lysine acetyl transferases/deacetylases (KATs/KDACs), protein kinases and phosphatases, and protein ubiquitin ligases (E3s). Provided that a clear therapeutic strategy can be envisaged, targeting these enzymes with small-molecule inhibitors can constitute a valid therapeutic approach for patients affected by cancer.[7] Along with writers and erasers, readers also play a key role in epigenetic control. For example, the methyllysine reader

Received: May 10, 2019
Revised: August 5, 2019
Published: August 7, 2019

Downloaded via UNIV OF NEW ENGLAND on October 22, 2019 at 22:00:54 (UTC).
See https://pubs.acs.org/sharingguidelines for options on how to legitimately share published articles.

© 2019 American Chemical Society

DOI: 10.1021/acs.biochem.9b00420
Biochemistry 2019, 58, 3634−3645

proteins are now established targets for cancer drug discovery and therapeutic development.[8]

SET (Suppressor of variegation, Enhancer of Zeste, Trithorax) and **MYND** (myeloid-Nervy-DEAF-1) domain containing protein **3** (**SMYD3**) is a lysine methyltransferase. It was discovered as a member of the RNA polymerase II complex and was first attributed with an activity toward histone H3 lysine amino acid residue 4 (H3K4).[9] Further studies have identified additional histone-based and non-nucleosomal substrates for SMYD3, including lysine 5 in histone H4 (H4K5),[10] lysine 831 in vascular endothelial growth factor receptor 1 (VEGFR1),[11] lysine 260 in mitogen activated protein kinase kinase kinase 3 (MAP3K2),[12] and lysine 175 in human epidermal growth factor receptor 2 (HER2).[13] This emerging intricate pattern of methylation targets, of both nuclear and cytoplasmic localization, endows SMYD3 with an important role as an epigenetic regulator. Many studies have highlighted a close correlation between an aberrant SMYD3 activity and the insurgence and progression of a plethora of malignancies. Currently, SMYD3 is a recognized actor in breast, lung, colorectal, hepatocellular, esophageal, and prostatic cancers.[14,15] For instance, it has been proven that SMYD3-mediated anomalous methylation of histone H3 promotes the recruitment of RNA Pol II and all of the associated transcription factors in pro-oncogenic regions, leading to liver and colon cancers.[14] In colorectal and lung carcinomas, MAP3K2 methylation by SMYD3 removes the inhibitory control of PPA2 protein, which in turn enhances proliferative pathways and overrides apoptosis signals by activation of the infamous MEK/ERK signaling cascade.[16,17]

Experimental evidence supports the idea that SMYD3 can be safely targeted for drug intervention, as its ablation in knockdown mice does not hamper the regular development of a healthy model organism.[12] Therefore, in the past decade, both academia and industry initiated research programs that aim to develop small molecule inhibitors of SMYD3. Tool compounds, differing in their inhibition mode, potency and bioavailability profiles, are now accessible on the market.[18−22] However, SMYD3 biology in the context of cancer is not fully understood yet. A recent elegant and far-reaching study of Thomenius et al. showed that SMYD3 activity was not related to autonomous cancer cell proliferation *in vitro* and that SMYD3 inhibition did not result in an appreciable cell death in cancer cell lines overexpressing this enzyme.[21] Nonetheless, SMYD3 remains a valid prospective target for oncotherapy, as *in vivo* data have shown a strong correlation between overexpression of this protein and a poor clinical prognosis.[23,24] This may be hypothesized to be a consequence of its role as a regulator of a tumor microenvironment, angiogenesis, or immune evasion.[12,23]

Translatability in drug discovery, i.e., the consistency of positive results from *in vitro* experiments and the corresponding clinical observations, heavily depends on the development of potent and highly selective chemical probes and on a deep comprehension of the disease biology on the preclinical level.[25,26] The critical step is arguably the characterization of the biological target of interest. To this aim, it is essential to have access to two resources: a valid procedure for high quality target production and reliable methods for ligand−target interaction studies, ideally complementary methods providing both structural and kinetic information.

In this work, we present an extensive platform for the biochemical characterization of SMYD3. A protocol for the production and crystallization of the enzyme was developed and standardized. A time-resolved surface plasmon resonance (SPR)-based biosensor assay was subsequently developed and employed for the characterization of SMYD3 interactions with small molecules and peptides encompassing amino acid sequences flanking the target lysine in naturally occurring SMYD3 substrates. Finally, a nonradioactive functional assay based on liquid chromatography coupled with mass spectrometry detection (LC-MS) was employed to investigate the methylation activity of the enzyme.

The methods and materials presented here can be generally employed to extract detailed information on the *in vitro* behavior of SMYD3 as a drug target and constitute valuable resources for identifying, prioritizing, and optimizing lead compounds that target SMYD3.

MATERIALS AND METHODS

Chemicals and Peptides. *S*-Adenosyl-methionine (SAM), *S*-adenosyl-homocysteine (SAH), and EPZ031686 (6-chloro-2-oxo-*N*-((1*R*,3*r*,5*S*)-8-(((1-(4,4,4-trifluorobutyl)piperidin-4-yl)methyl)sulfonyl)-8-azabicyclo[3.2.1]octan-3-yl)indoline-5-carboxamide) were all purchased from Sigma-Aldrich (Milan, Italy). 2-Amino-2-(hydroxymethyl)-1,3-propanediol (Tris), 2,2-bis(hydroxymethyl)-2,2′,2″-nitrilotriethanol (bis-Tris), sodium chloride (NaCl), Tween20, 4-(2-hydroxyethyl)-piperazine-1-ethanesulfonic acid (HEPES), dimethyl sulfoxide (DMSO), DL-dithiothreitol (DTT), magnesium chloride ($MgCl_2$), ethylenediaminetetraacetic acid (EDTA), and formic acid (FA) were also purchased from Sigma-Aldrich. All peptides but **11** (see Table 1, Results section) were purchased from Celtek Peptides with a stated purity >95%. Peptide **11** was a kind gift from Prof. Jan Kihlberg (Uppsala University, Sweden). The purity of the peptides was controlled and confirmed through LC-MS and MALDI-TOF MS.

Expression and Purification. SMYD3 cDNA was a kind gift from Dr. Nicolas Reynoird (Université de Grenoble Alpes, France). The gene was flanked with NdeI/XhoI endonucleases sites and subcloned into pET15b expression plasmid (Merck Millipore, USA). *E. coli* Rosetta 2 cells were employed for the expression. Cells were grown at 30 °C in Lysogeny Broth (LB) media, supplemented with ampicillin and chloramphenicol (100 and 35 μg/mL, respectively). Upon reaching optical density at 600 nm of 0.6, expression was induced at 20 °C with 0.4 mM IPTG for 16 h at RT, with an additional supplementation of the media with $ZnSO_4$ to 50 μM.

All of the following steps were performed at 4 °C, and all chromatographic steps were done using an Äkta Explorer FPLC system (Pharmacia, Sweden). Cells were lysed using a French press in buffer A (50 mM Tris, 300 mM NaCl, 10 mM imidazole, 5 mM β-mercaptoethanol (BME), pH 8.0), supplemented with 2 mM $MgCl_2$, 0.5 mM $CaCl_2$, 5 mM phenylmethylsulfofluoride (PMSF), and 10 μg/mL DNase I and RNase I (Hoffman-La Roche, Switzerland). The lysate was clarified and applied on a Ni^{2+}-NTA column. Elution was performed with a step gradient (buffer A, buffer B - same as A but with 300 mM imidazole) with an intermediate wash at 50 mM imidazole and a final elution at 300 mM. The IMAC fraction was desalted in a TBS buffer (50 mM Tris, 150 mM NaCl, 2 mM DTT, pH 8.0) using Sephadex G25 gel-filtration, mixed with human thrombin (0.5 catalytic unit per apparent mg of protein, Merck Millipore, USA), and incubated for 16 h.

DOI: 10.1021/acs.biochem.9b00420
Biochemistry 2019, 58, 3634−3645

Imidazole and NaCl concentrations were adjusted to 30 and 300 mM, respectively. The fraction was passed through a Ni^{2+}-NTA column and desalted into an anion exchange buffer C (50 mM Tris, 50 mM NaCl, 5 mM BME, pH 7.4). The protein was captured on Sepharose Q, eluted using a NaCl gradient at 150 mM salt concentration, buffer-exchanged into TBS, and concentrated to 9−12 mg/mL.

SMYD3 Crystallization. The protein was crystallized in a hanging drop manner, with a total drop volume of 2 μL, varying the protein-to-reservoir solution ratio as 1:1, 0.5:1.5, and 1.5:0.5. Protein was used at concentrations of 6−12 mg/mL in TBS buffer. Crystallization trials were performed at 20 °C, with a grid scan composed of 100 mM buffer, 50−100 mM magnesium acetate, 10−16% PEG3350 or 8−12% PEG8000, 0−20% DMSO, and 0 or 500 μM SAM; reservoir solution pH and the buffering component: 7.5 HEPES, 7.75, 8, 8.25, and 8.5 Tris, 8.75 and 9 bicine. Grown crystals were cryoprotected with 20% (v/v) 1,5-pentanediol or 10% (v/v) glycerol. Diffraction data was collected at synchrotron radiation sources in ESRF (Grennoble, France). Details of the crystallization trials are given in the Supporting Information.

Thermal Unfolding Assays. Thermal shift analysis was conducted either employing the solvatochromic dye SYPRO Orange (ThermoFisher Scientific, Netherlands) and a MJ MiniOpticon real-time PCR platform (BioRad Laboratories, USA) or intrinsic protein fluorescence using a TychoNT.6 nanoDSF instrument (NanoTemper Technologies, Germany). For the dye-assisted TSA, the protein was kept at 2 μM, and SYPRO Orange at 2× relative manufacturer concentration. Intrinsic fluorescence was recorded at 20 μM protein. Protein was prepared in a series of buffers, consisting of 100 mM of the buffering component and 200 mM NaCl: pH 5.0 and 5.5 sodium citrate, 6.0 and 6.5 MES, 7.0 bis-Tris, 7.5 HEPES, 8.0 Tris, 8.5 and 9 bicine, 9.5 ethanolamine. Additionally, the protein stability was assessed in TBS buffer supplemented with DMSO ranging from 0 to 10% (v/v).

Circular Dichroism Studies. Circular dichroism (CD) spectra were recorded on a Jasco-815 spectrometer (JASCO, Japan) using a 0.5 mm path length quartz cell (Hellma, Milan, Italy) and a Peltier temperature control unit. Measurements of a 12.5 μM solution of SMYD3 protein in TBS were performed in triplicate and averaged. The sample chamber was heated in steps with an increment of 2 °C, starting from 15 °C and terminating at 65 °C. Signals were acquired after 5 min of equilibration time. Spectroscopic parameters were set as follows: 2 nm spectral bandwidth, 2 s data integration time, and 0.5 nm data pitch.

Interaction Kinetic Analysis. All interaction kinetic experiments were conducted on flow SPR-based biosensors (BIAcore 3000, BIAcore T200 or BIAcore X100 from GE Healthcare, Sweden), using CM5 and Series S CM5 chips or Xantec CMD200 chips. The analysis temperature and running buffer composition, if not otherwise stated, were 15 °C and TBS buffer with 0.05% (v/v) surfactant Tween-20 supplemented with 2% DMSO (SPR assay buffer). The SPR data referencing and analysis were performed employing BIAeval 4.1 and BIAeval T200 3.0 software (GE Healthcare, Sweden) or gnuplot v. 5.2.

SMYD3 was diluted to 100 μg/mL in 10 mM bis-Tris, pH 7.0 buffer. The protein was immobilized in a buffer containing 10 mM HEPES, 150 mM NaCl, and 0.05% (v/v) Tween-20 at pH 7.4. Briefly, after activation of the surface via EDC/NHS injection (7 min), the protein solution was injected for 10 min (flow rate: 10 μL/min), whereafter the running buffer was changed to TBS. After a 12 h stabilization period, the sensing surface was ready for use. Whenever appropriate, the running buffer was supplemented with 1 μM SAM.

Alternatively, biotinylated $MAP3K2_{249-274}$ peptide [biotin−GGGG−DYDNPIFEKFGKGGTYPRRYHVSYH] was captured to a streptavidin-coated sensor chip (SA, BIAcore, Sweden). Aliquots of SMYD3 ranging from 50 to 0.78 μM (2-fold dilution series) were injected in the presence and in the absence of SAM in the running buffer. In this experimental setup, the analysis temperature was set to 25 °C.

Activity Studies. The methylation activity of SMYD3 was assessed using an end-point assay. 50 mM Tris, 4 mM $MgCl_2$, 2 mM DTT, 0.02% (v/v) Tween-20, 2% (v/v) DMSO, pH 8.0 was used as assay buffer. Enzymatic reactions were initiated by addition of the substrate peptide. When SAM was titrated, 0−50 μM, two-fold dilution series, 100 μM of peptide 1 were added to the assay buffer. When peptide 1 was titrated, 0−200 μM, two-fold dilution series, 50 μM of SAM where included in the assay buffer. The enzyme concentration was kept constant at 0.6 μM in a total reaction volume of 30 μL. Unless otherwise stated, assays were performed at 30 °C for 1 h. The methyl transferase activity was terminated by addition of 30 μL of a stop solution (H_2O/acetonitrile (AcCN)/formic acid (FA) 50/50/0.1 v/v/v). Eight μL of the resulting mixture was analyzed by LC-MS using the experimental conditions reported in the LC−MS analysis section. Nonlinear regression was performed in gnuplot v. 5.2 software, using the following equation:

$$v = \frac{V_{max}^{app}[S]^h}{K_{1/2} + [S]^h}$$

The parameter h was constrained to 1 when assuming a Michaelis−Menten model; it was held variable for data exhibiting sigmoidal kinetics.

Inhibition Analysis. EPZ031686[20] was used as a reference inhibitor to test the suitability of the developed assays for inhibition studies. A 10 mM stock solution of EPZ031686[20] was prepared in DMSO and, for the interaction kinetic experiments, further diluted to 200 μM in TBS buffer so that the final buffer composition matched the SPR assay buffer. Further dilutions, from 100 nM to 390 pM (4-fold dilution series), were prepared directly in the SPR assay buffer and injected in a single cycle kinetic (SCK) mode over the SMYD3-functionalized surface.

For IC_{50} determination, SMYD3 (5 μM) was preincubated in the absence and presence of EPZ031686 in the activity assay buffer (from 50 to 0.39 μM) at 23 °C for 1 h. The DMSO concetration was 2% (v/v). The methyltransferase activity was then determined by adding 5 μL of 300 μM SAM, 5 μL of 75 μM peptide **1**, and 14 μL of the activity assay buffer to 6 μL of preincubated mixtures. Final assay concentrations were as follows: SMYD3 1 μM, EPZ031686 from 10 to 0.08 μM, pep **1** 12.5 μM, SAM 50 μM, and the final percentage of DMSO 2% (v/v). After 1 h of incubation at 30 °C, SMYD3 was inactivated by adding 30 μL of stop solution consisting of H_2O/AcCN/FA (50/50/0.1, v/v/v). Ten μL was analyzed by LC-MS using the experimental conditions reported in the LC-MS analysis section. Experiments were performed in duplicate. Data were normalized using negative and positive controls: 2% DMSO only - 0% inhibition, 10 μM final concentration of EPZ031686 - 100% inhibition.

DOI: 10.1021/acs.biochem.9b00420
Biochemistry 2019, 58, 3634−3645

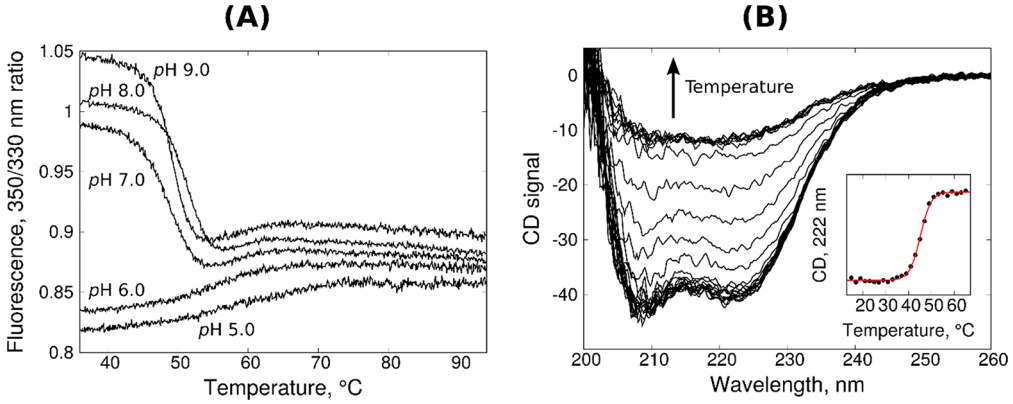

Figure 1. Analysis of SMYD3 stability. (A) Thermal unfolding at different pH values. Data were acquired by nanoDSF, monitoring changes in the intrinsic fluorescence of the protein (see Table S2 for T_m values). (B) CD spectra acquired at various temperatures (range 15−65 °C with 2 °C increment) in a standard TBS buffer. The inset shows the CD signal (ellipticity value) at 222 nm as a function of temperature, approximated with a three-parametric sigmoidal equation (fitted red line). The estimated melting temperature (T_m) was 45 °C.

IC_{50} values were determined from the dose−response inhibition curve using the two-parametric sigmoidal equation (2PL) with gnuplot v.5.2

$$\text{Inhibition (\%)} = 100 - \frac{100}{1 + ([I]/IC_{50})^h}$$

where h is a Hill-like coefficient and IC_{50} is the inhibitor concentration at half-maximal inhibition.

LC-MS Analysis. LC-MS analysis was carried out on an Agilent 1200 HPLC instrument equipped with a thermostated autosampler and a C4 reverse phase Jupiter 300 column (150 × 2 mm^2 i.d., 5 μm, 300 Å; Phenomenex, USA) kept at 60 °C, coupled to a Q-ToF mass-spectrometer with a Z-Spray ion source (Micromass, UK). For peptide **1**, mobile phases A (H_2O/AcCN/FA, 99/1/0.1) and B (AcCN/H_2O/FA, 99/1/0.1) were used to develop a solvent gradient as follows: 10−60% B over 2 min and 60% B for 3 min. When peptides **8** and **9** were analyzed, the mobile phase composition was changed to allow the retention of all of the peptides: phase A - H_2O/AcCN/FA/heptafluorobutyric acid (HFBA), 99/1/0.1/0.02; phase B - AcCN/H_2O/FA/HFBA, 99/1/0.1/0.02. Mass-spectrometric detection was performed under the following settings: source temperature - 100 °C, desolvation temperature - 250 °C, capillary voltage - 3.0 kV, cone voltage - 35 V. The mass chromatograms were recorded in total ion current (TIC), in the m/z range 500−1700, and the scan time was 1 s. The peptide's baseline-subtracted spectra were deconvoluted onto a true mass scale using the maximum entropy (MaxEnt1)-based software supplied with MassLynx software.

RESULTS

SMYD3 Overexpression, Purification, and Crystallization. SMYD3 cDNA was subcloned within the poly histidine reading frame of a pET15b plasmid. The final construct consisted of an N-terminal 6× His tag, followed by a thrombin cleavage site and the full-length SMYD3 protein. For the expression, the *E. coli* Rosetta 2 (a derivative of BL21(DE3)) strain was chosen, as the heterologous nature of the cDNA severely restricted the translation of the protein in rare-codon nonenriched strains.

The homogeneity of the isolated protein exceeded 98%, with an average yield of 5 mg of the pure protein from 1 L of culture. The high purity of the protein preparations was confirmed by mass spectrometry (MS) analysis (Figure S1).

Protein preparations were tested in a series of crystallization trials. The developed purification protocol resulted in a batch-to-batch reproducible crystallization of SMYD3. Crystallization conditions were found for two different crystal forms, differing both in their space groups and in the composition of the asymmetric unit (Table S1). After the initial analysis, the 3D structure of the enzyme appeared to be essentially identical to the published structures (data not shown). Detailed information regarding the crystallization procedures as well as diffraction abilities of the obtained SMYD3 crystals are given in the Supporting Information.

Protein Stability. In order to establish the best experimental conditions for studies involving SMYD3, its stability in different buffers and at different temperatures was explored. The melting temperature (T_m) in various media was initially evaluated using thermal unfolding assays. The pH stability was evaluated over the pH range 5.0−9.5, by detecting fluorescence changes upon binding of a solvatochromic dye to the protein (results not shown) or changes in the intrinsic fluorescence of tryptophan residues (Figure 1A). The highest T_m was observed at pH 8.0 in Tris-based buffer (Table S2). A typical unfolding profile was observed in the pH range 7.0−9.0, while, at lower pH values, SMYD3 exhibited a rapid loss of structural integrity. The enzyme thus appears to be stable at neutral and basic pH, up to 9.0. The SMYD3 T_m was also measured in DMSO-supplemented Tris buffer. No appreciable difference in T_m was detected up to 5% DMSO when compared to a DMSO-free Tris buffer (Table S2), indicating a good tolerance to this routinely used organic supplement.

To confirm that the protein had the expected secondary structure and to determine the T_m by an alternative method, circular dichroism spectroscopy (CD) was used. Data were first acquired at 15 °C in TBS buffer, matching the conditions to be used for biosensor experiments. The CD spectra showed intense negative bands at 208 and 222 nm, which are characteristic of secondary structures with a predominant α-helical content (Figure 1B).[27] Data could not be acquired at higher energy because of the strong absorption in this spectral region of buffer components. Subsequently, the sample chamber was gradually heated with an increment of 2 °C every 5 min. The signal intensity at 222 nm was plotted vs the corresponding temperature. The plot resulted in a sigmoidal

DOI: 10.1021/acs.biochem.9b00420
Biochemistry 2019, 58, 3634−3645

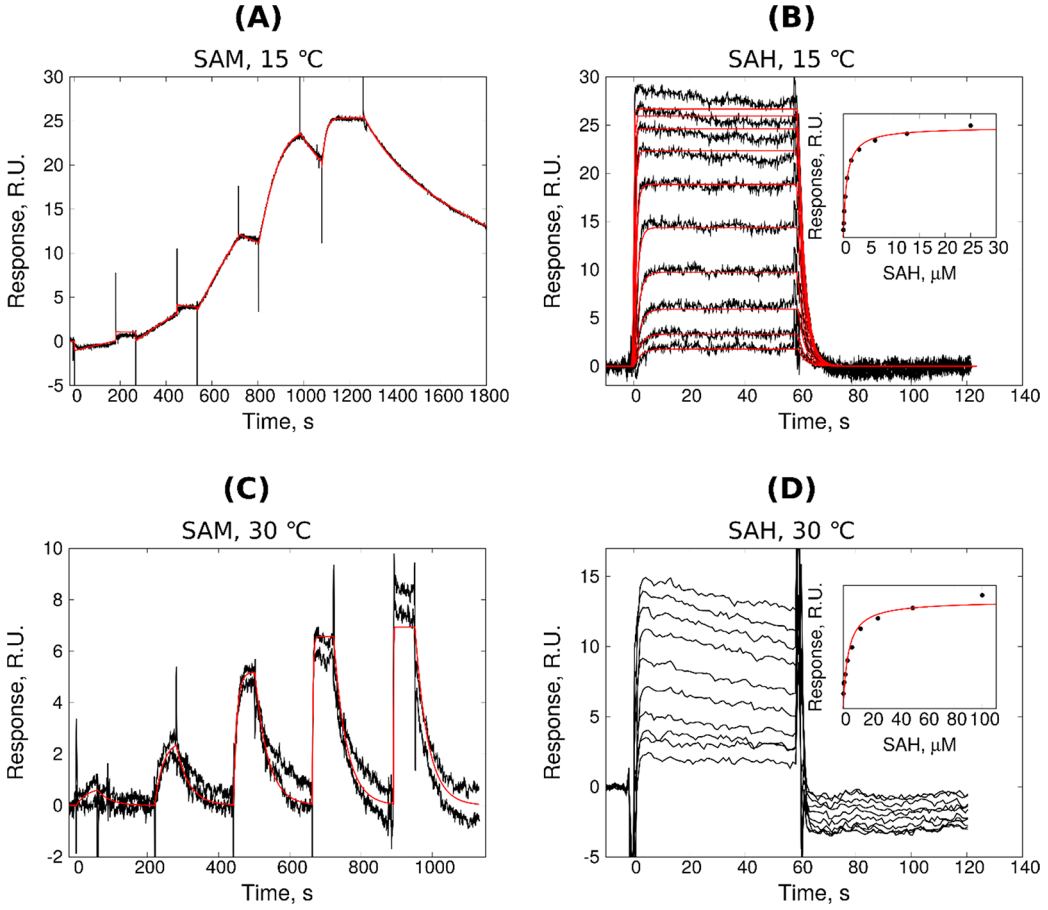

Figure 2. Kinetic analysis of SMYD3 interactions with natural small-molecule ligands at 15 °C (A and B) and 30 °C (C and D). Panels A, C - single-cycle kinetic titration of SAM. Panels B, D - SMYD3 interactions with SAH. Kinetic parameters were estimated from the interaction kinetic curves by global fitting using a 1:1 interaction kinetic model (A–C, red lines). K_D values were estimated by fitting a 1:1 interaction isotherm to dose–response curves extracted at steady state (B, D, insets, red lines).

curve, with a T_m value of 45 °C. The first signs of protein denaturation (onset temperature) were detected at 37–40 °C.

Interaction Kinetic Analysis. Interactions of SMYD3 with various model ligands were studied utilizing SPR-based biosensor technology. SMYD3-functionalized sensor surfaces were prepared using a slightly modified amine coupling protocol. An electrostatic preconcentration of the protein on the carboxymethyldextran-modified matrix was achieved in 10 mM bis-Tris buffer, pH 7.0, and high immobilization levels (9000–12000 resonance units, RU) could consistently be obtained.

To validate the functional integrity of the protein after immobilization and to refine the SPR-based assay, two natural small-molecule nucleoside ligands of SMYD3 were used: the methylation cofactor *S*-adenosylmethionine (SAM) and the enzymatic reaction product *S*-adenosylhomocysteine (SAH). Since the protein was purified as a complex with SAM, freshly prepared functionalized surfaces were flowed with SPR assay running buffer overnight to fully dissociate the copurified cofactor. Initial experiments showed that immobilized SMYD3 was functional and interacted with both nucleoside ligands. The experimental maximal responses (R_{max}) were 70% of the theoretical maximal responses estimated for these ligands.

Nevertheless, these experiments highlighted certain restrictions in the long term stability of the sensing surface. The functional integrity of the protein was dependent on the presence of thiol diexchange reagents in the assay buffer, as the response upon binding of ligands to the SMYD3 surface rapidly decreased in the absence of dithiothreitol (DTT) or 2-mercaptoethanol (BME) in the running buffer. The stability of the immobilized protein was also dependent on the analysis temperature. While the response of surfaces was considerably reduced within 24 h when used at 25 °C, thermostatting the analytical system at 15 °C stabilized the response over multiple days. To reflect the conditions envisaged for the *in vitro* enzyme activity analysis (see next section) and to allow a better correlation analysis between binding and activity data, SPR analyses were also performed at 30 °C on newly prepared surfaces. At this temperature, SMYD3-functionalized surfaces displayed a short life (<12 h), the experimental R_{max} dropped to ca. 30% of the expected R_{max}, and the sensorgram quality decreased accordingly; however, valuable information could still be extrapolated, at both a qualitative and a quantitative level.

Kinetic analysis of the interaction between the SMYD3-functionalized surfaces and SAM and SAH, performed at two different temperatures, showed that both ligands interacted with SMYD3 but with different kinetics (Figure 2). In order to accurately quantify the interactions, several experimental designs and data analysis procedures were used. The SMYD3–SAM interactions were analyzed employing a single-cycle kinetic approach,[28] due to the slow dissociation rate (i.e., a high stability of the complex). Association and dissociation rate constants (k_{on}, k_{off}) for the interactions were

DOI: 10.1021/acs.biochem.9b00420
Biochemistry 2019, 58, 3634–3645

Table 1. Peptides Representing Native Protein Substrates of SMYD3[a]

	parent protein$_{\text{peptide region}}$	peptide sequence	M_w (Da)	pI
1	MAP3K2$_{249-274}$	DYDNPIFEKFGK^{260}GGTYPRRYHVSYHH	3180	9.0
2	MAP3K2met1$_{249-274}$	DYDNPIFEKFGK$^{260}_{\text{met}}$GGTYPRRYHVSYHH	3198	8.9
3	MAP3K2Nleu$_{249-274}$	DYDNPIFEKFGN-leu^{260}GGTYPRRYHVSYHH	3165	7.8
4	MAP3K2$_{256-265}$	EKFGK^{260}GGTYP	1083	9.3
5	MAP3K2$_{258-263}$	FGK^{260}GGT	565	9.7
6	VEGFR1$_{820-845}$	WEFARERLKLGK^{831}SLGRGAFGKVVQAS	2891	11.7
7	VEGFR1$_{828-834}$	KLGK$^{831}_{\{\text{met2}\}}$SLG	729	10.8
8	H3K4$_{1-26}$	ARTK^{4}QTARKSTGGKAPRKQLATKAAR	2782	13.0
9	H4K5$_{1-26}$	SGRGK^{5}GGKGLGKGGAKRHRKVLRDNI	2703	12.5
10	CTD-HSP90	MEEVD	621	3.4
11	randomized	EQKARSRMAKT	1305	11.9

[a]Amino acid residues are enumerated according to their position in the full-length proteins. The lysine residues (or their analogues) are highlighted in bold. Molecular weights (M_w) and isoelectric points (pI) were calculated for peptides and given in the table.

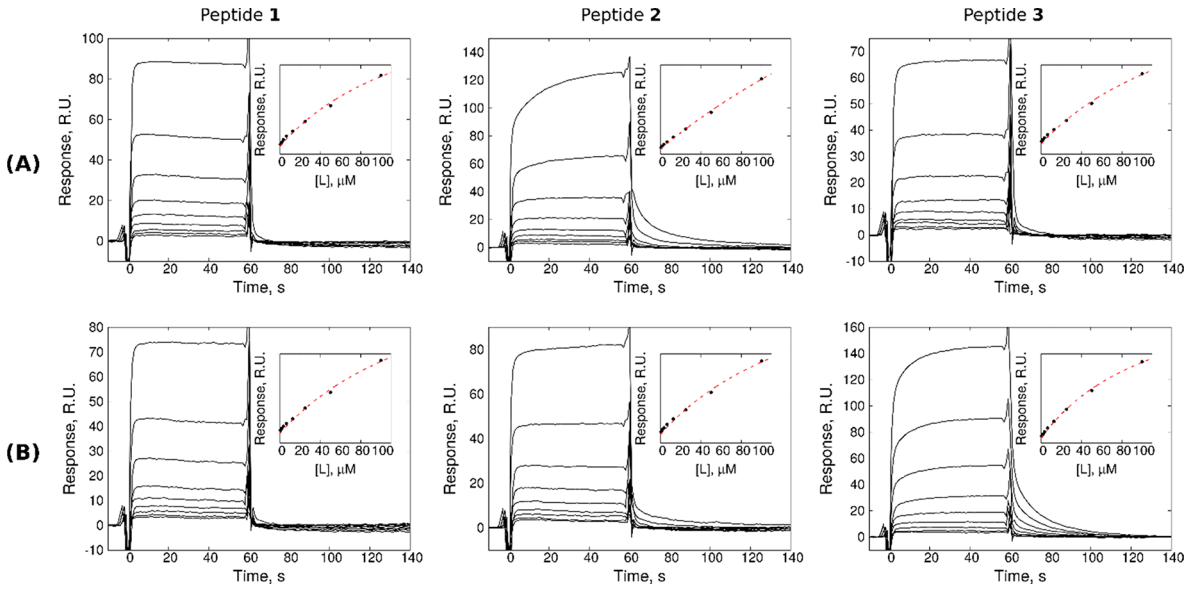

Figure 3. Interaction kinetic curves for immobilized SMYD3 and selected peptides (Table 1). Peptide solutions were prepared as 2-fold dilution series from 100 μM to 190 nM. Interactions were studied with apo-SMYD3 (A) and SAM-saturated SMYD3 (B). Insets show approximated interaction isotherms based on report points taken at the end of the injection and fitted with the Langmuir adsorption model (dashed red lines).

determined through global fitting of the interaction kinetic curves, while equilibrium dissociation constants (K_D) were derived from the ratio of the rate constants ($K_D = k_{off}/k_{on}$) or from fitting steady-state dose−response curves, in all cases assuming a 1:1 Langmuir-like interaction model (Figure 2, red curves).

At 15 °C (Figure 2A and C), the rate constants for the SMYD3−SAM interaction were $k_{on} = (1.4 \pm 0.2) \times 10^6$ M^{-1} s^{-1} and $k_{off} = (2.4 \pm 0.3) \times 10^{-3}$ s^{-1}, from which the corresponding $K_D = 1.7 \pm 0.3$ nM was derived, reflecting the thermodynamic stability of the complex. For the SMYD3−SAH interaction, rate constants were $k_{on} = (2.7 \pm 0.1) \times 10^6$ M^{-1} s^{-1}, $k_{off} = 1.6 \pm 0.9$ s^{-1}, and the derived $K_D = 611 \pm 2$ nM. The K_D determined by steady state analysis was 580 ± 47 nM. The >100-fold faster dissociation rate constant for the interaction between SMYD3 and the reaction product SAH, when compared to SAM, translated into a >100-fold lower affinity.

At 30 °C (Figure 2C and D), the parameters for the SMYD3−SAM interaction were $k_{on} = 9.7 \times 10^5$ M^{-1} s^{-1}, $k_{off} = 0.03$ s^{-1}, and $K_D = 31$ nM. The dissociation of SAH from the complex with SMYD3 was too fast for the quantification of the kinetic parameters. The steady-state analysis resulted in a thermodynamic K_D value of 3.5 μM. The association rate for SMYD3−SAM interaction was consequently somewhat slower at the higher temperature, but the dissociation rate was considerably faster, resulting in a 20-fold lower affinity. For SAH, the affinity was also lower at higher temperature, but a major effect on association or dissociation rates could not be pinpointed.

To examine the recognition events at the protein substrate binding site, the interactions were studied with a set of peptides containing a target lysine residue, or its mimic (Table 1). Peptides were selected on the basis of previous work by Fu et al.,[29] where the substrate preference for *in vitro* methyltransferase activity of SMYD3 was investigated through a scintillation counting-based assay in combination with crystallographic studies. We aimed to further clarify the substrate preference at the histone binding site of SMYD3 by a direct binding assay and to identify whether there is a minimum amino acid motif necessary to form a SMYD3−substrate complex. To this aim, we used five peptides based on the MAP3K2 protein sequence, differing in the length and structure of the acceptor lysine residue. Three variants of a 26-

DOI: 10.1021/acs.biochem.9b00420
Biochemistry 2019, 58, 3634−3645

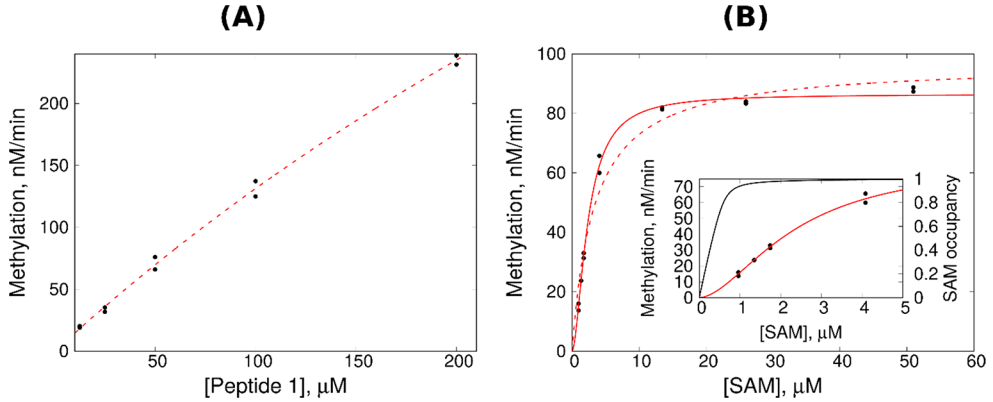

Figure 4. SMYD3 lysine methyltransferase activity analysis. (A) Peptide **1** in a 2-fold dilution series (0−200 μM) and 50 μM SAM. The data was analysed by non-linear regression using the Michaelis−Menten model, dashed red line. (B) SAM in a 2-fold dilution series (0−50 μM) and 100 μM of peptide **1**; inset - graph for low SAM concentrations. The data was analysed by using either Michaelis−Menten (dashed red line) or sigmoidal kinetic (red line) models. Inset - SAM saturation curve at low cofactor concentrations; solid black line, right axis - SAM site occupancy at given concentrations, calculated with a quadratic binding equation at 0.6 μM enzyme and SMYD3−SAM complex K_D = 30 nM.

aa-long peptide, with either a native lysine, a monomethylated lysine, and a lysine replaced by N-leucine were compared. A decapeptide and a hexapeptide, containing the native lysine, were also compared in order to establish the minimal length required for an adequate recognition.

Two peptides representing the binding site in VEGFR1 were also used: a 26-aa-long peptide with unmodified lysine residue and a 7-aa-long peptide with a dimethyl lysine. Two 26-aa-long peptides representing the N-terminal tails of the H3K4 and H4K5 proteins were included in the analysis. Finally, interaction with a pentapeptide representing the last five amino acids of the C-terminus domain (CTD) of HSP90 was also tested.

The peptides were injected over the SMYD3-functionalized surface in the presence or in the absence of SAM in the running buffer in order to determine the effect of the cofactor for the substrate binding. Generally, a maximal peptide concentration of 100 μM was used to avoid aggregation-related artifacts, as well as to reduce nonspecific interactions or precipitation-related issues.

Peptide **11** was included as a random amino acid sequence that was not expected to bind specifically to SMYD3. This peptide is characterized by two lysine residues and an alkaline isoelectric point (pI); it is therefore a suitable control for unspecific electrostatic interactions with the dextran matrix or negatively charged areas on the protein surface. When peptide **11** was injected over the sensor surface, no appreciable binding was detected. Analogously, peptides **4**, **5**, and **7**, representing two shorter analogues of MAP3K2 26-aa peptide and the shorter version of the VEGFR1 26-aa peptide, respectively, did not show any considerable interaction with the immobilized enzyme in the tested concentration range. All other peptides showed concentration-dependent signal responses, as expected for specific interactions (exemplified in Figure 3). However, the affinities were weak, as saturation would require significantly higher concentrations than the maximal peptide concentration used (100 μM). Moreover, the binding events were generally complex and deviated significantly from a simple interaction model. Under these conditions, quantification of the K_D values could lead to rather equivocal results and was not attempted.

It was found that SAM influences the recognition event and complex stabilization for certain peptides (Figure 3 and Figure S2). The interaction profile for peptide **1**, representing MAP3K2 with an unmodified lysine residue, showed a similar trend when measured in the presence and absence of SAM in the running buffer. However, the profiles for peptides **2**, **3**, **8**, and **9** (Figure 2 and Figure S2) were different under the two conditions. Peptide **2**, the methyl-lysine version of MAP3K2, formed a more stable complex with SMYD3 in the absence of SAM. Conversely, peptide **3**, the N-Leu substituted analogue of peptides **1** and **2**, formed complexes of higher stability with SMYD3 in the presence of the cofactor. For peptide **6**, representing the amino acid sequence mimicking the VEGFR1 binding motif, the responses recorded in the presence and in the absence of SAM were not significantly different. For peptide representatives of H3 and H4 N-tails, listed as **8** and **9**, respectively, higher responses in the presence of SAM were detected. However, the stability of the complexes remained roughly the same (Figure S2). Biosensor results obtained with shorter peptides of MAP3K2 and VEGFR1 (**4**, **5**, and **7**) suggest that amino acids far from the reactive lysine are necessary to form a complex with SMYD3, as no appreciable interaction was detected for the truncated variants.

No clear interaction was observed with peptide **10**, whose amino acid sequence consists of the five C-terminal amino acid residues of the molecular chaperone HSP90, a proposed interacting partner of SMYD3. Further analyses are necessary to clarify whether this minimum sequence is sufficient to evocate binding with the enzyme as reported by a previous study.[30]

To confirm the specificity of the observed interactions, the system was also reversed: peptide **1**, extended by glycine residues and capped with a biotin moiety from the N-terminus, was anchored to a streptavidin-coated surface at a level of approximately 70 RU, and SMYD3 was injected as an analyte. Also, SMYD3 interactions with the peptide-modified surface were assessed both in the presence and in the absence of SAM in the running buffer. Interaction profiles were comparable to those obtained in the experimental setup where SMYD3 was tethered to the surface, further confirming the specific low-affinity nature of the protein−peptide complexes (Figure S3).

Enzyme Activity Analysis. SMYD3 methyltransferase (MTase) activity was evaluated by measuring the degree of methylation of the target lysine residue of the peptides listed in Table 1. The use of electrospray (ESI)-LC-MS allowed the

DOI: 10.1021/acs.biochem.9b00420
Biochemistry 2019, 58, 3634−3645

unambiguous determination of the substrate modification from the deconvoluted mass spectrum. The identification of the non-, mono-, and dimethylated peptides was achieved measuring the characteristic mass shift of 14 and 28 Da, respectively, from the nonmethylated form (Figure S4).

The experimental conditions were optimized in order to obtain reproducible and reliable results. The presence of DMSO (2%, v/v) and Tween 20 (0.02%, w/v) was found to be crucial for the enzymatic activity and stability. Experiments were carried out at 30 °C, and the rate of methylation was determined in an end-point manner upon 1 h of incubation. Although the stability of SMYD3 at 30 °C is not suitable for long lasting experiments, the stability was suitable for these initial velocity-based activity assays. Indeed, upon 2 h of incubation at 30 °C, the decrease in activity was almost negligible (within 2%), and 95% of the initial activity was retained for 4 h. For quantitation purposes, the reaction rate was defined accounting for all methylated forms generated over the given time.

The enzymatic activity was characterized using peptide **1**, derived from the MAP3K2 protein (Table 1), and the methylation cofactor SAM. The choice of peptide **1** as the methylation substrate was based on previous work showing a specific SMYD3 activity with this protein *in vitro*.[29] However, the low affinity of peptide **1** for SMYD3, as already established in the interaction kinetic experiments using SPR (see above), did not allow saturation of the enzyme within an experimentally reasonable concentration range, Figure 4A. This behavior translates into a velocity curve that does not reach maximal velocity. In contrast, SAM titration resulted in a saturable velocity curve. Close inspection of the reaction rate saturation curve indicated a sigmoidal curvature. In a first approximation, data were analyzed utilizing both a standard Michaelis–Menten model and a sigmoidal enzyme kinetic model, as shown in Figure 4B. In the given experimental setup, a phenomenological analogue of the Michaelis–Menten constant, defined as $K_{1/2}$, was found to be 3.3 ± 0.4 μM.

To further characterize the substrate preferences of SMYD3, activity toward different peptidic substrates was assessed (Table 2). Only the un- and monomethylated MAP3K2$_{249-274}$ peptides (**1** and **2**) were significantly methylated (>15%), with only minor differences in the degree of methylation. The unmethylated peptide from VEGFR with a corresponding length (VEGFR1$_{824-845}$, peptide **6**) was only scarcely methylated under the developed experimental conditions. No methylation was detected for peptides derived from the N-tails of histones 3 and 4 (peptides **8** and **9**).

Table 2. SMYD3 Lysine Methyltransferase Activity Analysis with Different Substrate Peptides, Assessed Using a LC-MS End-Point Assay[a]

pep	substrate	% methylation
1	MAP3K2$_{249-274}$	16.8 ± 0.4
2	MAP3K2met1$_{249-274}$	19.8 ± 1.3
3	MAP3K2Nleu$_{249-274}$	n.d.
4	MAP3K2$_{256-265}$	n.d.
5	MAP3K2$_{258-263}$	n.d.
6	VEGFR1$_{820-845}$	1.7 ± 0.1
7	VEGFR1$_{828-834}$	n.d.
8	H3K4$_{1-26}$	n.d.
9	H4K5$_{1-26}$	n.d.

[a]Data from two independent experiments, each performed in duplicate, are reported as the mean of methylation percentage ± standard deviation. [b]n.d.: not detectable.

Inhibition Analysis. Interaction kinetic analysis revealed peculiar binding features for EPZ031686. However, a clear dose–response emerged from the sensorgrams, and saturation was reached within the experimental range of concentrations employed for the analysis, Figure 5A. Due to the extremely tight binding of EPZ031686, no theoretically reasonable model was suitable for estimation of the kinetic parameters for the interaction. By treating the dissociation event as a simple exponential decay, a k_{off} value below 8×10^{-5} s^{-1} and a relative $\tau_{1/2} > 2.4$ h could be estimated. These values indicate that the SMYD3–EPZ031686 complex is very stable. MS-based inhibition studies resulted in a clear dose–response inhibition curve (Figure 5B). Data analysis with a 2PL model resulted in $IC_{50} = 0.67 \pm 0.04$ μM, with an associated Hill-like slope factor of 1.7 ± 0.1.

DISCUSSION

An efficient protocol for the production of recombinant human SMYD3 in a pure, functional, and suitable for crystallization form was developed. For wide-ranging biochemical and biophysical studies of SMYD3, it was critical to also identify environmental conditions for handling the protein, ensuring good structural integrity and high functionality. Preliminary information was obtained from thermal unfolding experiments, which required a relatively simple sample preparation and limited experimental design that are two useful characteristics when multiple conditions need to be tested simultaneously. Solvatochromic dye-mediated and label-free approaches were both employed to study the most suitable buffer system for downstream work. The results showed that a higher thermal stability was achieved in a slightly alkaline environment (Figure 1A), with the highest stability observed at pH 8.0. The low stability of the protein at pH values below 7.0 can be attributed to the presence of zinc fingers within the protein structure, with a possible disruption of zinc-cation coordination upon protonation of the cysteine and histidine residues. Consequently, TBS buffer at pH 8.0 was employed as an assay buffer for the subsequent studies.

Further investigations of the thermal stability of the protein were conducted by means of CD spectroscopy, which allows the measurements of an asymmetric absorption of circularly polarized light by optically active molecules. As a result, distinct CD signatures can be correlated to the secondary structures in proteins, i.e., α-helix, β-strand, β-turn, and unordered regions. Although CD spectra could not be recorded at the highest energy wavelengths (180–200 nm) due to the high absorption of the buffer components, hampering the detailed definition of the secondary structure, the acquired CD spectra were informative. They showed negative bands at 208 and 222 nm, which are typical of proteins with a high α-helix content.[27] This finding is in agreement with the 3D structure of SMYD3, determined by X-ray crystallography, supporting the correct folding of the produced protein.[29] The melting temperature of SMYD3 was determined by CD analysis in TBS, in a temperature range between 15 and 65 °C. A clear loss of the α-helix signature with the increase in temperature was observed, culminating in a mostly unordered structure at the highest temperatures. The calculated T_m of 45 °C was in agreement with the values measured by FTSA. These results suggest that SMYD3 can be

DOI: 10.1021/acs.biochem.9b00420
Biochemistry 2019, 58, 3634–3645

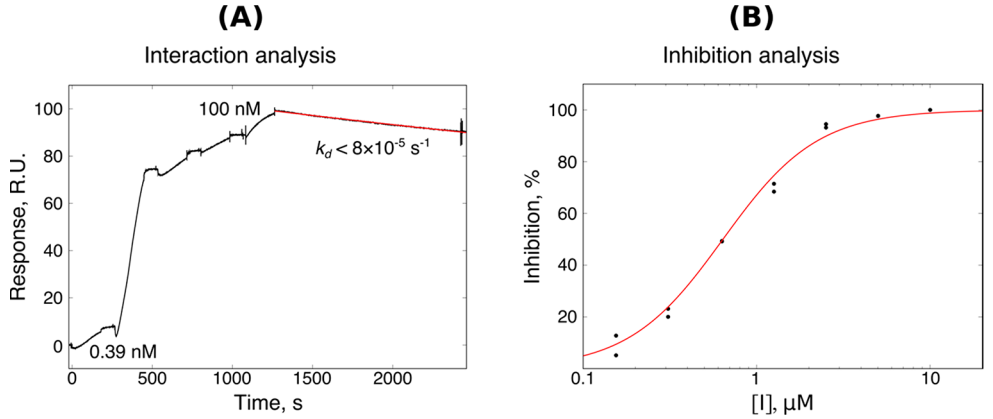

Figure 5. Validation of the designed SPR-biosensor-based interaction kinetic and methylation assays with a reference SMYD3 inhibitor EPZ031686. (A) Analysis of SMYD3−EPZ031686 interaction. The ligand was injected in SCK mode in 4-fold dilution series, spanning the concentration range from 100 to 0.39 nM. The decomposition of a very stable enzyme−inhibitor complex was evaluated with an analysis of the dissociation phase using one parametric exponential decay model (red line). (B) Inhibition analysis of EPZ031686. To quantify the apparent inhibition parameters, the activity data was fitted with the 2PL model (red line).

safely studied under the chosen conditions (30 °C and below), without a risk of damaging its structural integrity.

Screening procedures often require addition of organic solvents, typically DMSO, to the assay buffer to aid the solubility of poorly soluble compounds. A low percentage of DMSO is usually well tolerated by most biological entities; however, this behavior has to be carefully assessed on a case-by-case basis. SMYD3 was shown to tolerate a relatively high percentage of DMSO, suggesting that, when necessary, this organic cosolvent can be present at as high concentrations as 5%.

A sensitive and informative direct binding assay for characterization of interactions with SMYD3 was established. A standard amine coupling protocol for the preparation of sensor surfaces requires electrostatic preconcentration of the target protein at the sensorchip surface. Preconcentration is achievable when the dextran matrix and the protein bear opposite net charges. It is normally attained by employing low-ionic-strength solutions with a pH value between the pI of the protein and the pK_a of the carboxymethyl dextran matrix (ca. 3.6). For SMYD3, a pI of 6.8 can be assumed on the basis of its primary structure (https://web.expasy.org/protparam/). It suggests that coupling should be performed at a low pH value. Since the thermal unfolding analysis (Table S2) indicated that this condition causes protein denaturation, a slightly higher pH was used. It was found that the protein could be immobilized in a pH 7.0 bis-Tris-based coupling buffer.

The apparent surface binding capacity after the immobilization and the decay of surface functionality over time was evaluated using SAH as a reference ligand. Its interaction profile and fast dissociation kinetics render the compound particularly useful. This study revealed that the surface retained its functionality only up to 24 h when the SPR experiments were conducted at the standard temperature of 25 °C. This time frame is not sufficient for screening campaigns, which may require long experimental sessions. A lower temperature of 15 °C was therefore regularly used for the SPR-based interaction studies. At this temperature, the viability of the surface was extended to several days and was suitable for lengthy screening experiments.

A possible explanation for the poor stability of the sensor surface can be attributed to the redox stability of SMYD3. It has a high content of cysteine and methionine residues as compared to the average content in mammalian nonmembrane proteins, including structurally invariant cysteines involved in a formation of zinc fingers, with 5.4% of cysteines and 3.7% of methionine for SMYD3 against 2.1 and 2.0% on average.[31] This higher incidence increases the susceptibility of the thiols to oxidation to the corresponding sulfinic acids or methionine sulphones in a flow biosensor setup.

The functional assay partially correlated with the interaction kinetic analysis. Short peptides, i.e., peptides **4**, **5**, and **7**, were not methylated by SMYD3 (Table 2), as expected, since they were found to not be significantly bound by the protein in a direct interaction assay. However, although specific interactions with SMYD3 were detected for peptides **1**, **2**, **6**, **8**, and **9**, only peptides **1**, **2**, and **6** were functional as substrates, i.e., the 26-mer MAP3K2 (unmethylated and monomethylated) and 26-mer VEGFR1-based peptides. Thus, the formation of SMYD3−peptide complexes was orthogonally characterized by a low interaction efficiency and a subsequent poor methylation activity. Although this may not reflect the situation for native substrates, it influences the mechanism of the substrate recognition by SMYD3. It can be speculated that the low affinities are related to the highly flexible nature of peptides in solution. They can assume a number of interchanging conformations, of which only some can efficiently bind SMYD3 in a productive mode. Indeed, analysis of published X-ray structures of SMYD3 complexes with substrate-mimicking peptides (Figure 6) shows that, while the ε−N of the lysine residue locates exactly in the same position within the SMYD3 catalytic site for both MAP3K2 and VEGFR1-based peptides, the peptide backbones adopt different orientations. It is unlikely that recognition of the substrate proteins is achieved through the SMYD3 active site cavity exclusively. Considering the different nature of the proposed substrate proteins and an absence of a consensus between the flanking acceptor lysine residues, SMYD3 may not expose well-defined interaction hotspots on the active site surface. A proper orientation and positioning of the target lysine could be achieved through interactions with exosite regions, which

DOI: 10.1021/acs.biochem.9b00420
Biochemistry 2019, 58, 3634−3645

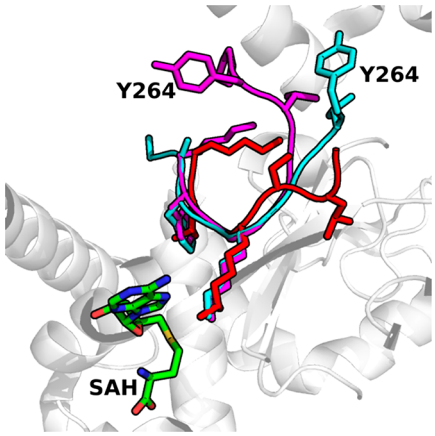

Figure 6. Crystallographic structures of SMYD3−peptide complexes: MAP3K2-based peptides 5EX0 (purple, aar 249−274, cocrystallized) and 5HQ8 (cyan, aar 250−264, cocrystallized), VEGFR1 (red, aar 820−845, soaked). MAP3K2-based peptides adopt different conformations in their C-terminal part; VEGFR1-based peptide also demonstrates a unique binding pose.

would constrain amino acid spatial arrangement and produce a productive binding pose.

Taking into account the peptidic nature of the substrates employed for this study, the results reported herein support a mechanistic model of SMYD3 methylation, which envisions a bi−bi random mechanism, Figure 7. The reaction scheme given in Figure 7 has already been proposed for other KTMases, including the closely related SMYD2, through evaluation of the product inhibition patterns.[32] To assess the validity of this model for SMYD3, the kinetics and stability of various forms of SMYD3, which possibly exist in a steady-state equilibrium during the *in vitro* activity experiments, were assessed for binary complexes of enzyme−substrate (Figure 2A and C, Figure 3A for peptides **1** and **2**), enzyme−product (Figure 2B and D, Figure 3A for peptide **2**), and tertiary complexes (Figure 3B, peptides **1** and **2**). As shown in the kinetic experiments for SMYD3−product interactions, the dissociation of the corresponding binary complexes is rapid. Additionally, a well-resolved mechanism and kinetics for the interactions within the cofactor binding site justify certain features of SMYD3 catalytic activity. A distinct difference between the interaction kinetics for the methylated and demethylated cofactor forms (Figure 2) was observed, as expected for a processive enzyme. Rapid rebinding of the methyl group donor promotes di- and three-methylation of the substrate protein, albeit its dissociation from the enzyme−product complex is slower than cofactor rebinding. As shown by biosensor experiments, this behavior is even more pronounced at 30 °C. For the cofactor, an increase in temperature did not translate into a significant change in the association rate constant k_{on}, while the off-rate constant value increased by 1 order of magnitude. Assuming a similar dependency for the methylation byproduct SAH and considering the change in its K_D value from 0.6 to ca. 3 μM, the SAH k_{off} value is expected to be significantly above 1 s^{-1} at a physiological temperature. Hence, a release of free enzyme from the binary enzyme−product complexes or cofactor recycling within the methylation site cannot be rate-limiting.

Similar association profiles for the interactions of the peptide substrate with SAM-saturated SMYD3 and with the free enzyme indicate that the methyl donor does not have a strong orthosteric effect on the active site. The selected peptide substrates do not discriminate between the two SMYD3 forms. This finding is in accordance with the random mechanism shown in Figure 7.

The nonhyperbolic dependency of the kinetic curve (Figure 4B) could be related to cofactor shortage rather than to a deviation from a classical Michaelis−Menten profile. Indeed, for low SAM concentrations, the product conversion within 60 min approached 100%. Initial velocity values for the beginning of the SAM saturation curve were not true initial rates and were significantly underestimated due to the cofactor depletion. Additionally, SAM, with a SMYD3 affinity of 30 nM, saturated completely the enzyme in a stoichiometric manner even at the lowest cofactor concentrations (Figure 4B, inset). Therefore, the enzyme was subject to only a few rapid catalytic turnovers at the given concentration range, possibly in a burst-phase manner, before the system could be valid to impose the steady-state conditions. Additionally, to increase the overall sensitivity of the assay and better determine enzyme activity parameters, model substrates endowed with higher specificity, as full-length proteins, might be necessary. To demonstrate the suitability of the assays for inhibitor testing, EPZ031686,[20] a known potent and selective inhibitor of SMYD3, was characterized in terms of direct interaction with the enzyme and inhibition capacity, Figure 5. The interaction kinetic assay reveled a tight binding profile associated with a long-lasting residence time, in accordance with the previously reported K_i = 1.1 nM.[20] Determination of IC_{50} resulted in an apparent value of approximately 0.7 μM. Considering the tight binding and [E] ≫ K_i, the IC_{50} value is expected to be of the same order of magnitude as the enzyme concentration. It also explains the increased curvature of the inhibition curve (Figure 5), with a Hill coefficient >1. A good match between the IC_{50} value and the enzyme concentration (0.7 and 1 μM, respectively) highlights the quality of the obtained protein preparations, with the assay conditions being similar to the active site titration experiment.

Overall, our study demonstrates that the peptide substrate chosen herein constitutes a valid tool to *in vitro* study SMYD3 behavior under different experimental conditions and for *in vitro* inhibition studies. Compared to the full-length substrates, peptides are easier to access and easier to handle, thus

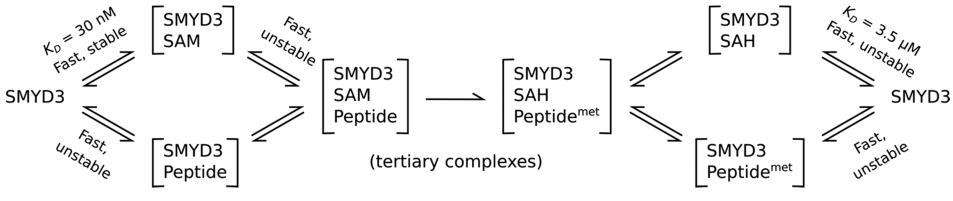

Figure 7. Generalized SMYD3 catalytic scheme for peptide-based substrates. The scheme shows a random bi−bi mechanism.

DOI: 10.1021/acs.biochem.9b00420
Biochemistry 2019, 58, 3634−3645

providing effective tools for biochemical studies of epigenetic enzymes.

CONCLUSIONS

The role that SMYD3 plays in many cancer types justifies detailed studies to unveil its biochemistry, as an understanding of the protein biology can aid the design of better chemical entities to be eventually developed into therapeutic agents. To reach these goals, both adequate amounts of the target enzyme and specific analytical methods are required. In this work, we addressed these points by developing an expression protocol, based on a rare-codon-enriched bacterial strain, which yields high amounts of active enzyme. Then, we developed a robust SPR-based assay to investigate binding events at the cofactor and substrate pockets.

A combination of the interaction kinetic data with data on enzyme activity obtained through an LC-MS-based assay supported a random bi−bi mechanism for the SMYD3 catalytic cycle, as already demonstrated for other KMTs. Our results showed that the interactions with the substrate binding pocket of SMYD3 is not very sequence specific and, although different peptides can specifically interact with SMYD3, only peptides based on a MAP3K2 sequence were effectively methylated by the enzyme, suggesting the necessity of exosite engagement for productive binding.

Overall, the set of assays described herein provides a base for ligand-binding screening through biosensor-based platforms and for inhibition studies through LC-MS analysis. The use of peptides as substrates can overcome the difficulty of handling and accessing full-length epigenetic substrates, providing nonetheless a valid means to investigate SMYD3.

ASSOCIATED CONTENT

Supporting Information

The Supporting Information is available free of charge on the ACS Publications website at DOI: 10.1021/acs.biochem.9b00420.

Details of crystallization trials and data collection; figures showing SMYD3 purity and sensorgrams for interactions between SMYD3 and peptides; ESI-MS data for SMYD3 activity assay; data for thermal stability analysis (PDF)

AUTHOR INFORMATION

Corresponding Author

*E-mail: helena.danielson@kemi.uu.se. Phone: +46704250103.

ORCID

U. Helena Danielson: 0000-0003-2728-0340

Author Contributions

E.F. and V.O.T. designed the study. V.O.T. and F.M. produced the protein. V.O.T. performed crystallization trials. E.F., V.O.T., and F.M. performed all biophysical experiments. E.F. and M.N. performed mass-spectrometric experiments. E.F. and V.O.T. analyzed the data and wrote the manuscript. C.B., A.D.R., M.B., and U.H.D. supervised the research. All of the authors contributed to the manuscript editing.

Author Contributions

∇E.F., V.O.T.: Contributed equally to the work

Funding

This work was financed by the Emilia Romagna region POR FSE 2014/2020 project ONCOPENTA, IG grant from Italian Association for Cancer Research N.19172, Erasmus+ Unipharma−graduates project, Marco Polo grant from school of pharmacy, biotechnology and physical education (2016), M.I.U.R. funding and European Community's Seventh Framework Programme (FP7/2007-2013) under BioStruct-X (Grant Agreement No. 283570). Financial support from the Swedish Research Council is gratefully acknowledged by U.H.D. (Grant No. D0571301).

Notes

The authors declare no competing financial interest.

ACKNOWLEDGMENTS

The authors are grateful to Dr. Helena Nordström and Dr. Eldar Abdurakhmanov (Science for Life Laboratories, Uppsala University, Sweden) for providing access to the BIAcore T200 instrument, Dr. Daniele Tedesco for precious comments on the circular dichroism analysis, and Dr. Doreen Dobritzsch for the help with the crystallographic trials. X-ray diffraction experiments were performed at the European Synchrotron Radiation Facility (ESRF, Grennoble, France); the authors are thankful to the staff of the beamline ID24 for their assistance with the crystal setup and data collection.

ACCESSION CODES

SMYD3	Q9H7B4; K13N variant (ENA ID: BAB86333.1, AAH31010.1)
MAP3K2	Q9Y2U5[249−274]; Q9Y2U5[256−265]; Q9Y2U5[258−263]
VEGFR1	P17948[820−845]; P17948[828−834]
Histone H3	P68431[2−-27]
Histone H4	P62805[2−27]
HSP90a	P07900[728−732]

REFERENCES

(1) Torre, L. A., Bray, F., Siegel, R. L., Ferlay, J., Lortet-Tieulent, J., and Jemal, A. (2015) Global cancer statistics, 2012. *Ca-Cancer J. Clin. 65*, 87−108.

(2) Hait, W. N. (2010) Anticancer drug development: the grand challenges. *Nat. Rev. Drug Discovery 9*, 253−254.

(3) Rodríguez-Paredes, M., and Esteller, M. (2011) Cancer epigenetics reaches mainstream oncology. *Nat. Med. 17*, 330−339.

(4) Bernstein, B. E., Meissner, A., and Lander, E. S. (2007) The Mammalian Epigenome. *Cell 128*, 669−681.

(5) Arrowsmith, C. H., Bountra, C., Fish, P. V., Lee, K., and Schapira, M. (2012) Epigenetic protein families: A new frontier for drug discovery. *Nat. Rev. Drug Discovery 11*, 384−400.

(6) Copeland, R. A. (2016) Epigenetic Medicinal Chemistry. *ACS Med. Chem. Lett. 7*, 124−127.

(7) Copeland, R. A., Olhava, E. J., and Scott, M. P. (2010) Targeting epigenetic enzymes for drug discovery. *Curr. Opin. Chem. Biol. 14*, 505−510.

(8) Milosevich, N., and Hof, F. (2016) Chemical Inhibitors of Epigenetic Methyllysine Reader Proteins. *Biochemistry 55* (11), 1570−83.

(9) Hamamoto, R., Furukawa, Y., Morita, M., Iimura, Y., Silva, F. P., Li, M., Yagyu, R., and Nakamura, Y. (2004) SMYD3 encodes a histone methyltransferase involved in the proliferation of cancer cells. *Nat. Cell Biol. 6*, 731−740.

(10) van Aller, G. S., Reynoird, N., Barbash, O., Huddleston, M., Liu, S., Zmoos, A. F., McDevitt, P., Sinnamon, R., Le, B. C., Mas, G., Annan, R., Sage, J., Garcia, B. A., Tummino, P. J., Gozani, O., and Kruger, R. G. (2012) Smyd3 regulates cancer cell phenotypes and catalyzes histone H4 lysine 5 methylation. *Epigenetics 7*, 340−343.

(11) Kunizaki, M., Hamamoto, R., Silva, F. P., Yamaguchi, K., Nagayasu, T., Shibuya, M., Nakamura, Y., and Furukawa, Y. (2007)

DOI: 10.1021/acs.biochem.9b00420
Biochemistry 2019, 58, 3634−3645

The lysine 831 of vascular endothelial growth factor receptor 1 is a novel target of methylation by SMYD3. *Cancer Res. 67*, 10759−65.
(12) Mazur, P. K., Reynoird, N., Khatri, P., Jansen, P. W. T. C., Wilkinson, A. W., Liu, S., Barbash, O., Van Aller, G. S., Huddleston, M., Dhanak, D., Tummino, P. J., Kruger, R. G., Garcia, B. A., Butte, A. J., Vermeulen, M., Sage, J., and Gozani, O. (2014) SMYD3 links lysine methylation of MAP3K2 to Ras-driven cancer. *Nature 510*, 283−287.
(13) Yoshioka, Y., Suzuki, T., Matsuo, Y., Tsurita, G., Watanabe, T., Dohmae, N., Nakamura, Y., and Hamamoto, R. (2017) Protein lysine methyltransferase SMYD3 is involved in tumorigenesis through regulation of HER2 homodimerization. *Cancer Med. 6*, 1665−1672.
(14) Giakountis, A., Moulos, P., Sarris, M. E., Hatzis, P., and Talianidis, I. (2017) Smyd3-associated regulatory pathways in cancer. *Semin. Cancer Biol. 42*, 70−80.
(15) Rajajeyabalachandran, G., Kumar, S., Murugesan, T., Ekambaram, S., Padmavathy, R., Jegatheesan, S. K., Mullangi, R., and Rajagopal, S. (2017) Therapeutical potential of deregulated lysine methyltransferase SMYD3 as a safe target for novel anticancer agents. *Expert Opin. Ther. Targets 21*, 145−157.
(16) Colón-Bolea, P., and Crespo, P. (2014) Lysine methylation in cancer: SMYD3-MAP3K2 teaches us new lessons in the Ras-ERK pathway. *BioEssays 36*, 1162−1169.
(17) Deuker, M. M., and Mcmahon, M. (2014) Cancer biology: enzyme meets a surprise target. *Nature 510* (7504), 225−226.
(18) Peserico, A., Germani, A., Sanese, P., Barbosa, A. J., Di Virgilio, V., Fittipaldi, R., Fabini, E., Bertucci, C., Varchi, G., Moyer, M. P., Caretti, G., Del Rio, A., and Simone, C. (2015) A SMYD3 Small-Molecule Inhibitor Impairing Cancer Cell Growth. *J. Cell. Physiol. 230*, 2447−2460.
(19) Van Aller, G. S., Graves, A. P., Elkins, P. A., Bonnette, W. G., McDevitt, P. J., Zappacosta, F., Annan, R. S., Dean, T. W., Su, D. S., Carpenter, C. L., Mohammad, H. P., and Kruger, R. G. (2016) Structure-Based Design of a Novel SMYD3 Inhibitor that Bridges the SAM-and MEKK2-Binding Pockets. *Structure 24*, 774−781.
(20) Mitchell, L. H., Boriack-Sjodin, P. A., Smith, S., Thomenius, M., Rioux, N., Munchhof, M., Mills, J. E., Klaus, C., Totman, J., Riera, T. V., Raimondi, A., Jacques, S. L., West, K., Foley, M., Waters, N. J., Kuntz, K. W., Wigle, T. J., Scott, M. P., Copeland, R. A., Smith, J. J., and Chesworth, R. (2016) Novel Oxindole Sulfonamides and Sulfamides: EPZ031686, the First Orally Bioavailable Small Molecule SMYD3 Inhibitor. *ACS Med. Chem. Lett. 7*, 134−138.
(21) Thomenius, M. J., Totman, J., Harvey, D., Mitchell, L. H., Riera, T. V., Cosmopoulos, K., Grassian, A. R., Klaus, C., Foley, M., Admirand, E. A., Jahic, H., Majer, C., Wigle, T., Jacques, S. L., Gureasko, J., Brach, D., Lingaraj, T., West, K., Smith, S., Rioux, N., Waters, N. J., Tang, C., Raimondi, A., Munchhof, M., Mills, J. E., Ribich, S., Porter Scott, M., Kuntz, K. W., Janzen, W. P., Moyer, M., Smith, J. J., Chesworth, R., Copeland, R. A., and Boriack-Sjodin, P. A. (2018) Small molecule inhibitors and CRISPR/Cas9 mutagenesis demonstrate that SMYD2 and SMYD3 activity are dispensable for autonomous cancer cell proliferation. *PLoS One 13*, No. e0197372.
(22) Fabini, E., Manoni, E., Ferroni, C., Del Rio, A., and Bartolini, M. (2019) Small-molecule inhibitors of lysine methyltransferases SMYD2 and SMYD3: current trends. *Future Med. Chem. 11*, 901−921.
(23) Fei, X., Ma, Y., Liu, X., and Meng, Z. (2017) Overexpression of SMYD3 Is Predictive of Unfavorable Prognosis in Hepatocellular Carcinoma. *Tohoku J. Exp. Med. 243*, 219−226.
(24) Sarris, M. E., Moulos, P., Haroniti, A., Giakountis, A., and Talianidis, I. (2016) Smyd3 Is a Transcriptional Potentiator of Multiple Cancer-Promoting Genes and Required for Liver and Colon Cancer Development. *Cancer Cell 29*, 354−366.
(25) Rezaee, R., and Abdollahi, M. (2017) The importance of translatability in drug discovery. *Expert Opin. Drug Discovery 12*, 237−239.
(26) Shih, H. P., Zhang, X., and Aronov, A. M. (2018) Drug discovery effectiveness from the standpoint of therapeutic mechanisms and indications. *Nat. Rev. Drug Discovery 17*, 19−33.
(27) Greenfield, N. J. (2006) Using circular dichroism spectra to estimate protein secondary structure. *Nat. Protoc. 1*, 2876−90.
(28) Karlsson, R., Katsamba, P. S., Nordin, H., Pol, E., and Myszka, D. G. (2006) Analyzing a kinetic titration series using affinity biosensors. *Anal. Biochem. 349*, 136−147.
(29) Fu, W., Liu, N., Qiao, Q., Wang, M., Min, J., Zhu, B., Xu, R. M., and Yang, N. (2016) Structural basis for substrate preference of SMYD3, a SET domain-containing protein lysine methyltransferase. *J. Biol. Chem. 291*, 9173−9180.
(30) Brown, M. A., Foreman, K., Harriss, J., Das, C., Zhu, L., Edwards, M., Shaaban, S., and Tucker, H. (2015) C-terminal domain of SMYD3 serves as a unique HSP90-regulated motif in oncogenesis. *Oncotarget 6*, 4005−19.
(31) Gaur, R. K. (2014) Amino acid frequency distribution among eukaryotic proteins. *IIOAB J. 5*, 6−11.
(32) Ferguson, A. D., Larsen, N. A., Howard, T., Pollard, H., Green, I., Grande, C., Cheung, T., Garcia-Arenas, R., Cowen, S., Wu, J., Godin, R., Chen, H., and Keen, N. (2011) Structural basis of substrate methylation and inhibition of SMYD2. *Structure*, Elsevier Ltd.

DOI: 10.1021/acs.biochem.9b00420
Biochemistry 2019, 58, 3634−3645